

**SANDIA REPORT**

**SAND2006-7319**

Unlimited Release

Printed December 2006

**Final LDRD Report for Projects # 52797  
and # 93362: Rational Understanding  
and Control of the Magnetic Behavior of  
Nanoparticles**

Z. John Zhang

Prepared by  
Sandia National Laboratories  
Albuquerque, New Mexico 87185 and Livermore, California 94550

Sandia is a multiprogram laboratory operated by Sandia Corporation,  
a Lockheed Martin Company, for the United States Department of Energy's  
National Nuclear Security Administration under Contract DE-AC04-94-AL85000.

Approved for public release; further dissemination unlimited.



Issued by Sandia National Laboratories, operated for the United States Department of Energy by Sandia Corporation.

**NOTICE:** This report was prepared as an account of work sponsored by an agency of the United States Government. Neither the United States Government, nor any agency thereof, nor any of their employees, nor any of their contractors, subcontractors, or their employees, make any warranty, express or implied, or assume any legal liability or responsibility for the accuracy, completeness, or usefulness of any information, apparatus, product, or process disclosed, or represent that its use would not infringe privately owned rights. Reference herein to any specific commercial product, process, or service by trade name, trademark, manufacturer, or otherwise, does not necessarily constitute or imply its endorsement, recommendation, or favoring by the United States Government, any agency thereof, or any of their contractors or subcontractors. The views and opinions expressed herein do not necessarily state or reflect those of the United States Government, any agency thereof, or any of their contractors.

Printed in the United States of America. This report has been reproduced directly from the best available copy.

Available to DOE and DOE contractors from  
U.S. Department of Energy  
Office of Scientific and Technical Information  
P.O. Box 62  
Oak Ridge, TN 37831

Telephone: (865) 576-8401  
Facsimile: (865) 576-5728  
E-Mail: [reports@adonis.osti.gov](mailto:reports@adonis.osti.gov)  
Online ordering: <http://www.doe.gov/bridge>

Available to the public from  
U.S. Department of Commerce  
National Technical Information Service  
5285 Port Royal Rd  
Springfield, VA 22161

Telephone: (800) 553-6847  
Facsimile: (703) 605-6900  
E-Mail: [orders@ntis.fedworld.gov](mailto:orders@ntis.fedworld.gov)  
Online order: <http://www.ntis.gov/help/ordermethods.asp?loc=7-4-0#online>



# **Final LDRD Report for Projects # 52797 and # 93362: Rational Understanding and Control of the Magnetic Behavior of Nanoparticles**

Z. John Zhang  
School of Chemistry & Biochemistry,  
Georgia Institute of Technology  
Atlanta, Georgia 30332

## **Abstract**

This is the final LDRD report for projects # 52797 and # 93362 that funded a five year research program directed by Prof. Z. John Zhang at the Georgia Institute of Technology Chemistry Department. Prof. Zhang was awarded this funding after winning a Presidential Early Career Award in Science and Engineering (PECASE) in 2001 with Sandia as the DOE sponsoring lab. The project PI was Blake Simmons and the PM was Alfredo Morales.

The page intentionally left blank

# Contents

Abstract .....	3
Contents .....	5
1. Introduction .....	7
2. Accomplishments .....	9
2.1 Synthesis of magnetic nanoparticles and correlations of their magnetic properties with quantum couplings .....	9
2.2 Surface effect on the magnetic properties of nanoparticles .....	11
2.3 Coating magnetic nanoparticles with a layer of polymer or silica .....	13
References .....	15
Distribution .....	17
Internal .....	17
External .....	17

## List of Figures

Figure 1.	There are two types of lattice sites (A and B) for cation occupancy, and the A sites have a tetrahedral symmetry while B sites have an octahedral symmetry (Fig.1). Usually, $M^{2+}$ and $Fe^{3+}$ cations can be found on both sites. ....	7
Figure 2.	Transmission electron microscopy (TEM) micrograph (Fig.2) shows magnetic nanoparticles of $CoFe_2O_4$ with a fairly uniform size of $\sim 7.9$ nm. ...	9
Figure 3.	TEM micrographs with the scale bar as 50 nm. The size in Panel (a) and (b) is $5.2\pm 1.1$ and $7.9\pm 0.5$ nm spherical $CoFe_2O_4$ nanocrystals, respectively. Panel (c) and (d) show $9.1\pm 0.5$ and $10.9\pm 0.6$ nm cubic $CoFe_2O_4$ nanocrystals, respectively. Panel (e) is $11.8\pm 1.3$ nm spherical $CoFe_2O_4$ nanocrystals. Panel (f), as a representative histogram, shows the size distribution of cubic nanocrystals in Panel (d) after measuring over 400 nanocrystals. The inset in Panel (f) displays the aspect ratios of cubic nanocrystals in Panel (c) and (d).....	10
Figure 4.	The TEM micrograph for the coated products presented in Figure 4 shows individual $MnFe_2O_4$ particles coated with a thin polystyrene shell. ...	14
Figure 5.	Figure 5 displays a TEM micrograph of $MnFe_2O_4$ -silica core-shell nanoparticles. ....	14

## List of Tables

Table 1.	Percentage decrease in coercivity from surface modification by <i>para</i> substituted benzoic acid ligands with respect to the native 4 nm $MnFe_2O_4$ nanoparticles. ....	12
Table 2.	Percentage decrease in coercivity from surface modification by benzene derivatives with respect to the native 4 nm $MnFe_2O_4$ nanoparticles.....	12
Table 3.	Percentage decrease in coercivity of variable sized modified nanoparticles with respect to the corresponding native 4, 12, and 25 nm $MnFe_2O_4$ nanoparticles .....	12

# Rational Understanding and Control of the Magnetic Behavior of Nanoparticles

## 1. Introduction

Understanding and controlling the magnetic properties of nanoparticles is of great interest not only for fundamental science researchers but also for realizing high impact applications such as magnetic drug delivery, biomedical imaging, and thermal stability of high-density data storage. The magnetic behavior of nanoparticles and its origin are not yet well understood. The magnetic properties of materials are partially dictated from magnetic interactions at an atomic level, including electron spin-spin (S-S) and electron spin-orbital angular momentum (L-S) couplings at crystal lattices. Since these couplings are determined by atomic placement on crystal lattice sites, the magnetic properties of materials can be controlled by manipulating crystal chemistry.

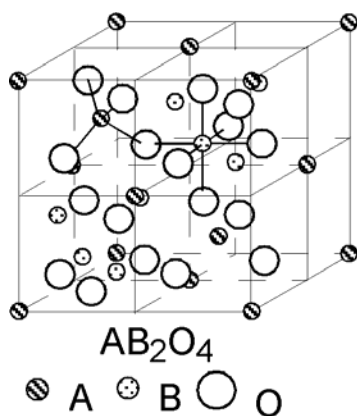


Figure 1

Spinel ferrites,  $MFe_2O_4$  ( $M = Mn, Mg, Zn, Co, Fe$  etc.) are among the most important magnetic materials and have a rich crystal chemistry. Due to the high compositional and structural flexibility, spinel ferrites offer great opportunities for studying the correlation between the magnetic properties and crystal chemistry and also for designing and fine-tuning the magnetic properties of nanoparticles. There are two types of lattice sites (A and B) for cation occupancy, and the A sites have a tetrahedral symmetry while B sites have an octahedral symmetry (Fig.1). Usually,  $M^{2+}$  and  $Fe^{3+}$  cations can be found on both sites .

The page intentionally left blank

## 2. Accomplishments

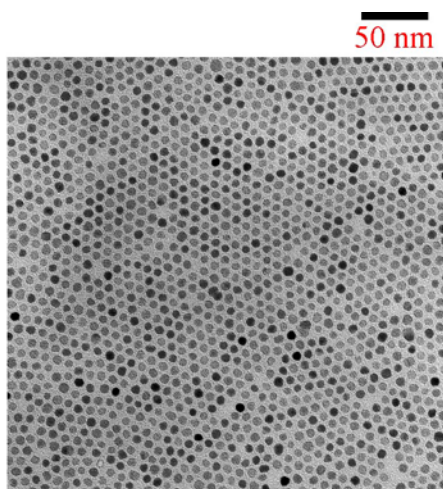
We have been working on the correlations between the magnetic quantum couplings and the magnetic properties of nanoparticles. Although it still is impossible to conduct ab initio calculation on the exchange couplings and spin-orbital couplings in solid state systems, the ligand field theory has allowed us to gain a great deal of insight into the correlations between quantum couplings and magnetic properties of nanoparticles. The ligand field theory in combination with the fundamental principles of magnetism points the research directions as well as provides a framework for interpretations in our magnetic nanoparticle research.

Here I summarize our accomplishments along three broad lines.

- 1) Successful development of new chemical methods for synthesizing high quality, monodispersed spinel ferrite magnetic nanoparticles and control of the shape of nanoparticles.
- 2) Clear understanding of surface effects on the magnetic properties of spinel ferrite nanoparticles.
- 3) Successful development of magnetic nanoparticles coated with polymer and silica shells.

### 2.1 Synthesis of magnetic nanoparticles and correlations of their magnetic properties with quantum couplings

By combining non-hydrolytic reaction with seed-mediated growth, high quality and monodisperse spinel cobalt ferrite,  $\text{CoFe}_2\text{O}_4$  nanocrystals can be synthesized with a highly controllable shape of nearly spherical or almost perfectly cubic. The shape of the nanocrystals can also be reversibly interchanged between spherical and cubic morphology through controlling nanocrystal growth rate. Transmission electron microscopy (TEM) micrograph (Fig.2) shows magnetic nanoparticles of  $\text{CoFe}_2\text{O}_4$  with a fairly uniform size of  $\sim 7.9$  nm.



$\text{CoFe}_2\text{O}_4$  Nanoparticles,  $7.9 \pm 0.5$  nm

**Figure 2**

The general synthesis strategy is using coordination compounds of iron(III) and cobalt(II) acetylacetonate,  $\text{Fe}(\text{acac})_3$  and  $\text{Co}(\text{acac})_2$  as precursors in a non-hydrolytic process to synthesize  $\text{CoFe}_2\text{O}_4$  spherical nanocrystals with a mean diameter of 5 nm. Such 5 nm nanocrystals then serve as seeds to grow larger spherical or cubic nanocrystals in the seed-mediated growth process.

In a typical synthesis, a mixture of 2 mmol  $\text{Co}(\text{acac})_2$ , 40 mL phenyl ether, 20 mmol 1,2-hexadecanediol, 10 mL oleic acid and 10 mL oleylamine was heated to  $140^\circ\text{C}$  followed by a droplet addition of 4 mmol  $\text{Fe}(\text{acac})_3$  in 20 mL phenyl ether solution. The temperature of the non-hydrolytic reaction was then increased quickly to  $260^\circ\text{C}$  and the mixture was kept to reflux for 30 min before cooled down to room temperature. After adding ethanol and centrifuging, spherical  $\text{CoFe}_2\text{O}_4$  nanocrystals with a diameter of 5 nm were obtained.

Such 5 nm nanocrystals were used as seeds to grow 8 or 9 nm spherical nanocrystals in the solution of  $\text{Co}(\text{acac})_2$  and  $\text{Fe}(\text{acac})_3$  precursors. For instance, to produce 8 nm spherical nanocrystals, 100 mg of seeds were used in a particle growth solution consisting of 1 mmol  $\text{Co}(\text{acac})_2$ , 2 mmol  $\text{Fe}(\text{acac})_3$ , 10 mmol 1-octadecanol, 5 mL oleic acid, and 5 mL oleylamine. Then, the solution temperature was raised to 260 °C at a rate of 10-15 degree/min and kept to reflux at 260 °C for 30 min. The nanocrystals precipitated out after ethanol was added. The nanoparticulate samples were suspended in hexane for transmission electron microscopy (TEM) studies.

The 5 nm nanocrystals served as the seeds for the seed-mediated growth as the second step of the synthesis for the nanocrystals with a diameter of 8 or 9 nm. The size of the nanocrystals was controlled through the ratio between the quantity of nanocrystalline seeds and the amount of precursors in the solution for seed-mediated growth. The growth procedures described in the experimental section have generated the sample consisted of 8 nm spherical nanocrystals together with a tiny fraction of nanocrystals having a ~5 nm diameter. Monodisperse 8 nm nanocrystals (Fig.3b) were obtained after small amount of acetone was added into the hexane suspension of as-grown nanoparticulate sample.

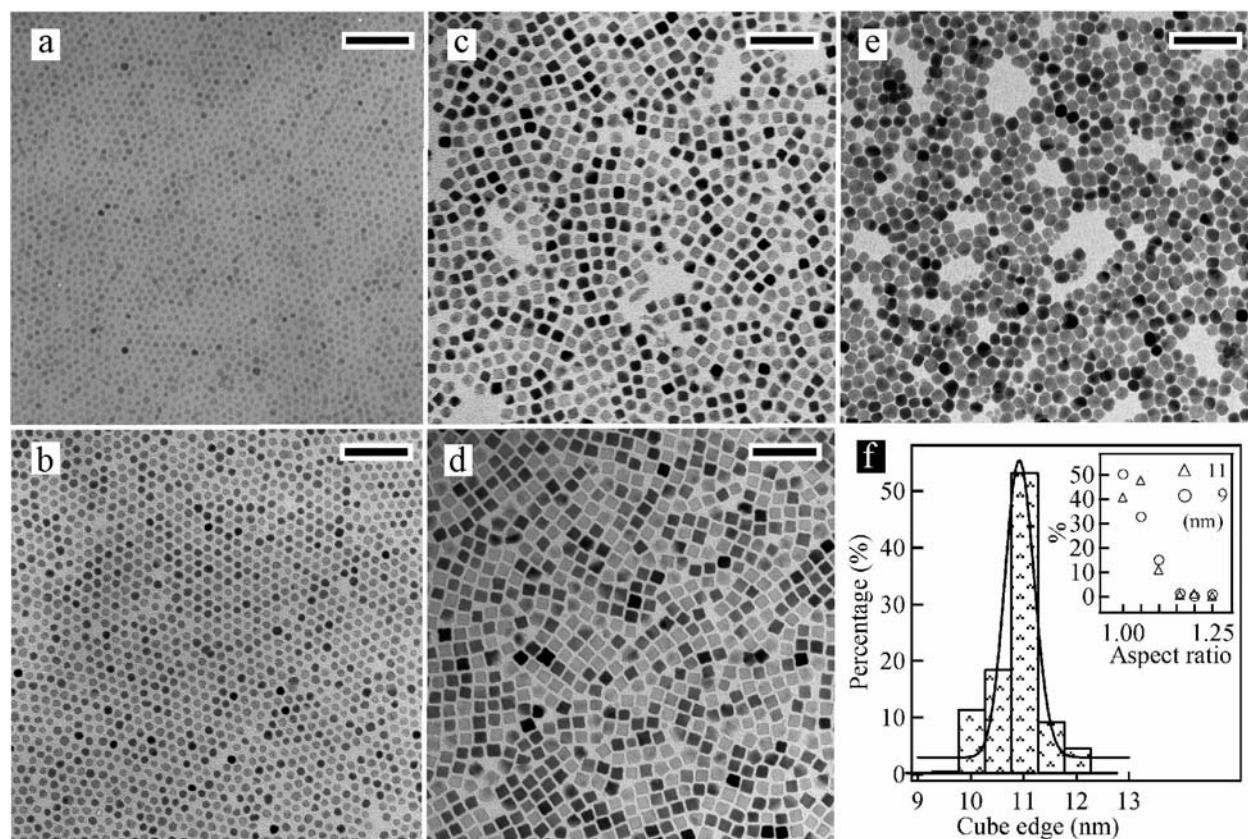


**Figure 3.** TEM micrographs with the scale bar as 50 nm. The size in Panel (a) and (b) is  $5.2 \pm 1.1$  and  $7.9 \pm 0.5$  nm spherical  $\text{CoFe}_2\text{O}_4$  nanocrystals, respectively. Panel (c) and (d) show  $9.1 \pm 0.5$  and  $10.9 \pm 0.6$  nm cubic  $\text{CoFe}_2\text{O}_4$  nanocrystals, respectively. Panel (e) is  $11.8 \pm 1.3$  nm spherical  $\text{CoFe}_2\text{O}_4$  nanocrystals. Panel (f), as a representative histogram, shows the size distribution of cubic nanocrystals in Panel (d) after measuring over 400 nanocrystals. The inset in Panel (f) displays the aspect ratios of cubic nanocrystals in Panel (c) and (d).

Monodisperse nanocrystals with a 9 nm diameter can be obtained using the same procedures but with increased concentration of precursors in the particle growth solution. Although nanocrystals with a larger diameter can also be prepared with 5 nm seeds, the quality of nanocrystals in term of size distribution usually deteriorated. Therefore, monodisperse nanocrystals with larger diameters were typically produced by incrementally increasing the size of nanoparticulate seeds. For instance, 8 nm nanocrystals were used in seed-mediated growth to synthesize monodisperse nanocrystals with a diameter of 10 or 12 nm.

It is very intriguing that the shape of  $\text{CoFe}_2\text{O}_4$  nanocrystals can be tuned to cubic during the seed-mediated growth process. Growth reaction parameters such as heating rate, temperature, reaction time, ratio of seed to precursors, and ratio of oleic acid to oleylamine have been systematically studied for the control of size and shape of nanocrystals. The results indicated that heating rate and growth temperature control the shape of  $\text{CoFe}_2\text{O}_4$  nanocrystals. Using the same 5 nm spherical seeds and the same growth solution as for the preparation of 8 or 9 nm spherical nanocrystals, cubic  $\text{CoFe}_2\text{O}_4$  nanocrystals were produced with an edge length of 8 or 9 nm when the temperature was raised only to 210 °C at a rate of 2-3 degree/min. The product was mainly monodisperse nanocubes (Fig.3c). A very tiny fraction of the product consisted of ~5 nm spherical nanocrystals, which can be easily separated from the cubes through addition of acetone into the hexane suspension. By using 8 nm spherical seeds, nanocubes with an edge length of 10 or 11 nm have been produced (Fig.3d).

Furthermore, the magnetic studies show that the blocking temperature, saturation and remanent magnetization of nanocrystals are solely determined by the size regardless the spherical or cubic shape. However, the shape of the nanocrystals is a dominating factor for the coercivity of nanocrystals due to the effect of surface anisotropy. Such magnetic nanocrystals with distinct shapes possess tremendous potentials in fundamental understanding of magnetism and in technological applications of magnetic nanocrystals for high-density information storage.

## 2.2 Surface effect on the magnetic properties of nanoparticles

In addition, Spinel ferrite  $\text{CoCr}_x\text{Fe}_{2-x}\text{O}_4$  nanoparticles over a compositional range  $0 < x < 1$  were synthesized using a reverse micelle microemulsion method. This method provided excellent control over the composition and gave a reasonable size distribution. Upon increased Cr substitution, the blocking temperature, saturation magnetization, remnant magnetization, and coercivity were all found to decrease. The compositional influence upon the magnetic properties is consistent with the effects on the magnetocrystalline anisotropy energy by weakened coupling between electron spin and the angular momentum of electron orbital (L-S). The results from size dependent magnetic studies on the nanoparticles with a composition of  $\text{CoCr}_{0.5}\text{Fe}_{1.5}\text{O}_4$  were found to agree well with the Stoner-Wohlfarth model. In order to understand the influence of surface interactions upon the magnetic properties of magnetic nanoparticles, the surface of manganese ferrite,  $\text{MnFe}_2\text{O}_4$ , nanoparticles have been systematically modified with a series of *para*-substituted benzoic acid ligands ( $\text{HOOC-C}_6\text{H}_4\text{-R}$ ;  $\text{R} = \text{H}, \text{CH}_3, \text{Cl}, \text{NO}_2, \text{OH}$ ) and substituted benzene ligands ( $\text{Y-C}_6\text{H}_5$ ,  $\text{Y} = \text{COOH}, \text{SH}, \text{NH}_2, \text{OH}, \text{SO}_3\text{H}$ ). The coercivity of magnetic nanoparticles decreases up to almost 50% upon the coordination of the ligands on the nanoparticle surface while the saturation magnetization has increased (Table 1 & 2).

**Table 1. Percentage decrease in coercivity from surface modification by *para* substituted benzoic acid ligands with respect to the native 4 nm MnFe<sub>2</sub>O<sub>4</sub> nanoparticles.**

Ligand	pK <sub>a</sub>	H <sub>C</sub> (G)	% H <sub>C</sub> decrease
native 4nm MnFe <sub>2</sub> O <sub>4</sub>	---	1563	---
<i>p</i> – hydroxybenzoic acid ( <b>R</b> = OH)	4.48	808	48.3
<i>p</i> – toluic acid ( <b>R</b> = CH <sub>3</sub> )	4.27	871	44.3
benzoic acid ( <b>R</b> = H)	4.19	885	43.4
<i>p</i> – chlorobenzoic acid ( <b>R</b> = Cl)	3.98	975	37.6
<i>p</i> – nitrobenzoic acid ( <b>R</b> = NO <sub>2</sub> )	3.42	1058	32.3

**Table 2. Percentage decrease in coercivity from surface modification by benzene derivatives with respect to the native 4 nm MnFe<sub>2</sub>O<sub>4</sub> nanoparticles**

Ligand	H <sub>C</sub> (G)	% H <sub>C</sub> decrease
native 4 nm MnFe <sub>2</sub> O <sub>4</sub>	1563	---
benzenethiol ( <b>Y</b> = SH)	814	47.9
benzoic acid ( <b>Y</b> = COOH)	885	43.4
benzenesulfonic acid ( <b>Y</b> = SO <sub>3</sub> H)	1005	35.7
aniline ( <b>Y</b> = NH <sub>2</sub> )	1091	30.2
phenol ( <b>Y</b> = OH)	1171	25.1

The percentage coercivity decrease of the modified nanoparticles with respect to the native nanoparticles strongly correlates with the crystal field splitting energy (CFSE)  $\Delta$  evoked by the coordination ligands. The ligand inducing largest CFSE results in the strongest effect on the coercivity of magnetic nanoparticles. The change on magnetic properties of nanoparticles also correlates with the specific coordinating function group bound onto the nanoparticle surface. The correlations suggest the decrease in spin-orbital couplings and surface anisotropy of magnetic nanoparticles due to the surface coordination. Such surface effects clearly show the dependence on the size of nanoparticles (Table 3).

**Table 3. Percentage decrease in coercivity of variable sized modified nanoparticles with respect to the corresponding native 4, 12, and 25 nm MnFe<sub>2</sub>O<sub>4</sub> nanoparticles**

Ligand	4 nm MnFe <sub>2</sub> O <sub>4</sub>		12 nm MnFe <sub>2</sub> O <sub>4</sub>		25 nm MnFe <sub>2</sub> O <sub>4</sub>	
	H <sub>C</sub> (G)	% H <sub>C</sub> decrease	H <sub>C</sub> (G)	% H <sub>C</sub> decrease	H <sub>C</sub> (G)	% H <sub>C</sub> decrease
native MnFe <sub>2</sub> O <sub>4</sub>	1563	---	799	---	354	---
<i>p</i> - hydroxybenzoic acid	808	48.3	678	15.2	310	12.4
<i>p</i> - toluic acid	871	44.3	690	13.6	313	11.5
benzenesulfonic acid	1005	35.7	598	25.1	301	15.0
aniline	1091	30.2	602	24.7	314	11.3
phenol	1171	25.1	767	4.0	345	2.5

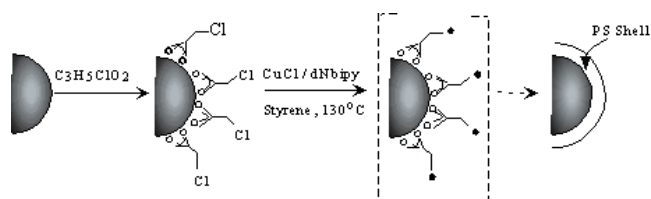
At larger nanoparticle sizes, the overall surface influences are greatly weakened, and therefore these slight variations may not be observable. When the electronic nature of the binding moiety is more markedly changed, as in the case of the benzene derivatives in which the atom attached to the surface is different, the electronic effects are likely stronger and hence the variation in surface effects on the magnetic properties are still able to be observed in larger nanoparticles.

The extent of coercivity decrease correlates with the capability of inducing crystal field splitting energy by surface coordination ligand. Such correlations can be understood from the fact that the spin-orbit couplings of magnetic cations decrease with increasing crystal field splitting energy evoked by the coordination ligands. Certainly, the magnetic response of nanoparticles to the surface modification elucidates the quantum origins of magnetic properties such as hysteresis. Furthermore, the effects of surface coordination chemistry upon the magnetic nanoparticles are important for the design of magnetoelectronic devices that make use of spin exchange at surfaces. The surface effects should also have impacts on the potential use of surface magnetism for tuning the magnetic properties of nanoparticles, and on the development of bioligand-modified magnetic nanoparticles for biomedical applications.

### 2.3 Coating magnetic nanoparticles with a layer of polymer or silica

Modification of nanoparticle surfaces with a thin shell material is a challenge in fundamental research and also of significance in applications. It can reduce the increased surface reactivity that occurs upon reduction of size, and tune the optical, magnetic, or catalytic properties of nanoparticles. The core-shell type materials have a wide range of applications from ordered composite films for electronic applications to biomedical applications such as biocompatibility and drug delivery.

We have successfully coated  $\text{MnFe}_2\text{O}_4$  nanoparticles with polystyrene using atom transfer radical polymerization (ATRP) yielding a core-shell particle with size  $< 15$  nm. The following scheme shows the synthesis procedure for polystyrene coated  $\text{MnFe}_2\text{O}_4$  nanoparticles using ATRP method.



Photoacoustic surface infrared spectroscopy of the dried product confirms the presence of polystyrene. Characteristic peaks of polystyrene at  $2700\text{-}3500\text{ cm}^{-1}$ ,  $1000\text{-}1400\text{ cm}^{-1}$ , and  $700\text{ cm}^{-1}$  are observed in the coated product spectra that were not present in the spectra of the  $\text{MnFe}_2\text{O}_4$  nanoparticle precursors. Transmission electron microscopy (TEM) studies were performed on a JEOL 100C, operating at 100kV. Nanoparticles were suspended in toluene and dispersed onto a holey carbon grid for the TEM studies. Particle sizes were determined by manually counting over 100 particles. The TEM micrograph for the coated products presented in Figure 4 shows individual  $\text{MnFe}_2\text{O}_4$  particles coated with a thin polystyrene shell. The average  $\text{MnFe}_2\text{O}_4$  nanoparticle size was  $9.3 \pm 1.5$  nm with a  $3.4 \pm 0.8$  nm polystyrene shell. The few aggregates are likely due to chain entanglement during solvent evaporation.

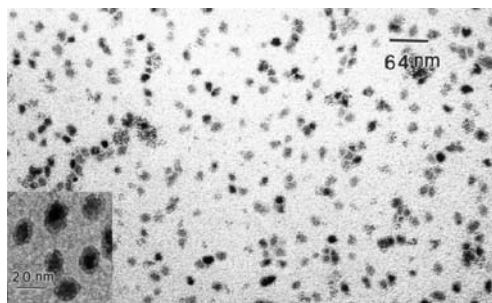


**Figure 4**

Such an atom transfer radical polymerization route works very well to form polystyrene shell on nanoparticulate  $\text{MnFe}_2\text{O}_4$  and provides magnetic core/shell nanoparticles with size  $<15$  nm. Magnetic studies show a decrease in coercivity, which is consistent with the reduction of magnetic surface anisotropy upon polymer coating. Certainly the magnetic core of these core/shell nanoparticles can be selected depending upon the desired superparamagnetic properties for specific applications such as in data storage and MRI contrast enhancement. Moreover, the resulting core/shell nanoparticles are within the biological size restrictions and may potentially be modified for a particular biospecificity.

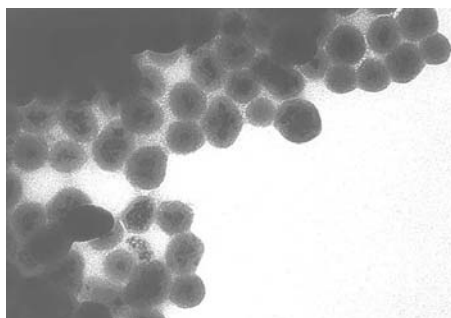


**Figure 5**

We have also used a reverse micelle microemulsion method with the surfactant polyoxyethylene(5)nonylphenyl ether (Igepal CO-520) to prepare silica coated magnetic spinel ferrite nanoparticles ( $\text{MFe}_2\text{O}_4$ ;  $\text{M} = \text{Co}, \text{Mn}, \text{Fe}, \text{Ni}, \text{Mg} \dots$ ) with a tunable core. High quality spinel ferrite nanoparticles with a narrow size distribution (typically 9-15%) are prepared prior to silica shell formation. Such two separate steps for the synthesis of core-shell nanostructure allow great flexibility in the selection of the magnetic core chosen for its desired magnetic response. There is no need for re-inventing the reaction procedure when a different magnetic core is chosen. Figure 5 displays a TEM micrograph of  $\text{MnFe}_2\text{O}_4$ -silica core-shell nanoparticles. Inset shows higher magnification of a silica-ferrite core-shell nanoparticle with a diameter of 72 nm. Magnetic measurements show a reduction in saturation and remanent magnetization that is attributed to the reduced portion of magnetic material per gram of core-shell nanoparticles. The coercivity of  $\text{MnFe}_2\text{O}_4$ -silica core-shell nanoparticles decreases a small amount from the value in native magnetic nanoparticles, which was not observed for the  $\text{CoFe}_2\text{O}_4$ -silica core-shell system. This decrease is likely due to the larger contribution of the surface anisotropy to the total anisotropy of  $\text{MnFe}_2\text{O}_4$  nanoparticles. Using the reverse micelle microemulsion method, a wide range of spinel ferrite nanoparticle cores can easily be coated with a silica shell. Such a method increases the potential for development of tunable magnetic silica for magneto-electronic and biomedical applications.

Overall, we are very grateful to the support from Sandia National Laboratory. Such supports have enabled our research group to stay at the forefront of the worldwide research on magnetic properties at nanometer scale and to contribute to strengthening the leadership role of U.S. science establishment in the world.

## References

The following is a list of peer-reviewed scientific papers that have been published as a result of this project:

1. “Synthesis of  $\text{CoCrFe}_2\text{O}_4$  nanoparticles using microemulsion methods and size dependent studies of their magnetic properties”, C.R. Vestal, Z.J. Zhang, *Chem. Mater.* **2002**, *14*, 3817.
2. “Atom transfer radical polymerization of polystyrene shell on  $\text{MnFe}_2\text{O}_4$  magnetic nanoparticles”, C.R. Vestal, Z.J. Zhang, *J. Am. Chem. Soc.* **2002**, *124*, 14313.
3. “Normal micelle synthesis and characterization of  $\text{MgAl}_2\text{O}_4$  spinel nanoparticles”, C.R. Vestal, Z.J. Zhang, *J. Solid State Chem.* **2003**, *175*, 59.
4. “Effects of surface coordination chemistry on the magnetic properties of  $\text{MnFe}_2\text{O}_4$  spinel ferrite nanoparticles”, C.R. Vestal, Z.J. Zhang, *J. Am. Chem. Soc.* **2003**, *125*, 9828.
5. “Synthesis and magnetic characterization of Mn and Co spinel ferrite-silica nanoparticles with tunable magnetic core”, C.R. Vestal, Z.J. Zhang, *Nano Lett.* **2003**, *3*, 1739.
6. “Magnetic spinel ferrite nanoparticles from microemulsion synthesis” C.R. Vestal, Z.J. Zhang, *Int. J. of Nanotechnology*, **2004**, *1-2*, 240.
7. “Quantum couplings and magnetic properties of  $\text{CoCr}_x\text{Fe}_{2-x}\text{O}_4$  ( $0 < x < 1$ ) spinel ferrite nanoparticles synthesized with reverse micelle method”, M. Han, C.R. Vestal, Z.J. Zhang, *J. Phys. Chem. B*, **2004**, *108*, 583.
8. “Shape control and associated magnetic properties of spinel cobalt ferrite nanocrystals”, Q. Song, Z.J. Zhang, *J. Am. Chem. Soc.* **2004**, *126*, 6164.
9. “Effects of interparticle interactions upon the magnetic properties of  $\text{CoFe}_2\text{O}_4$  and  $\text{MnFe}_2\text{O}_4$  nanocrystals”, C.R. Vestal, Q. Song, Z.J. Zhang, *J. Phys. Chem. B*, **2004**, *108*, 18222.
10. “Correlation between Spin-Orbital Coupling and the Superparamagnetic Properties in Magnetite and Cobalt Ferrite Spinel Nanocrystals”, Q. Song, Z.J. Zhang, *J. phys. Chem. B* **2006**, *110*, 11205.

The page intentionally left blank

# Distribution

**Internal:**

**External:**

